

## Generation of nitric oxide gradients in microfluidic devices for cell culture using spatially controlled chemical reactions

Ying-Hua Chen, Chien-Chung Peng, Yung-Ju Cheng, Jin-Gen Wu,  
and Yi-Chung Tung<sup>a)</sup>

*Research Center for Applied Sciences, Academia Sinica, Taipei 11529, Taiwan*

(Received 15 August 2013; accepted 25 October 2013; published online 7 November 2013)

In this paper, we develop a microfluidic device capable of generating nitric oxide (NO) gradients for cell culture using spatially controlled chemical reactions. NO plays an essential role in various biological activities, including nervous, immune, and cardiovascular systems. The device developed in this paper can control NO gradients without utilizing expensive and hazardous high purity NO gas sources or direct addition of NO donors. Consequently, the device provides an efficient, cost-effective, robust, and stable platform to generate NO gradients for cell culture studies. In the experiments, NO gradients are first characterized using a NO-sensitive fluorescence dye, and cell experiments using aortic smooth muscle cells are conducted. The results demonstrate that the device can alter the intracellular NO concentrations and further affect the  $\text{Ca}^{2+}$  concentration oscillation for the cells. The device developed in this paper provides a powerful platform for researchers better study the biological roles of NO and its spatial distribution using *in vitro* cell models with minimal instrumentation. © 2013 AIP Publishing LLC. [<http://dx.doi.org/10.1063/1.4829775>]

### INTRODUCTION

Nitric oxide (NO) is crucial to human bodies for its multiple biological functions, such as vasodilation, neurotransmission, and nonspecific host defense.<sup>1–4</sup> NO serves as an intercellular messenger, regulating the blood flow and modulating synaptic plasticity in neurons.<sup>2</sup> For non-specific host defense, NO, which is cytotoxic against intracellular pathogens, is produced by macrophages to kill tumor cells. In spite of all these advantages, NO can also be very harmful to bodies when it is overproduced.<sup>1,2</sup> For instance, during cerebral ischemia, the NO concentration can be greatly elevated to  $4\text{ }\mu\text{M}$ , which is 100-fold higher than that in normal conditions.<sup>2</sup> Through its reaction with superoxide, the overproduced NO will generate a significant amount of peroxynitrite, which is remarkably stable and highly toxic.<sup>2</sup> Consequently, in order to fully understand the role of NO on cells, it is highly desired to control microenvironments capable of generating various NO concentrations for cell culture.

In recent decades, several approaches have been exploited to control NO concentrations for biomedical applications. The current methods to control NO mainly rely on direct introduction of NO from gas cylinders, or direct chemical additions into culture medium.<sup>2,5–10</sup> However, NO in high concentration is extremely toxic when it reacts with oxygen and forms nitrogen dioxide ( $\text{NO}_2$ ). Therefore, the instrumentation is often overly complex and bulky and requires professional operation when gas cylinder is exploited. In contrast, NO generation via chemical addition can greatly simplify the instrument setup. However, the reactivity of NO donor is usually larger than that of NO; therefore, it is challenging to avoid the influence of chemical additions on the cells.<sup>2</sup> For instance, a NO donor, sodium nitroprusside (SNP), will inhibit cell proliferation by attacking thiols.<sup>11</sup> Furthermore, the effects of cellular-scale spatial distribution of NO, which

<sup>a)</sup> Author to whom correspondence should be addressed. Electronic mail: [tungy@gate.sinica.edu.tw](mailto:tungy@gate.sinica.edu.tw). Tel.: +886 2 2789 8000 ext 67; Fax: +886 2 2782 6680

exists in a number of physiological microenvironments,<sup>12</sup> on cellular behaviors have not been well studied due to limitations from current methods.

Recently, various microfluidic cell culture devices have been developed due to the desired properties of microfluidics.<sup>13–18</sup> These devices are capable of reconstituting various physiologically meaningful chemical and physical microenvironments for *in vitro* cell studies. In addition, due to better control in both spatial and temporal domains, microfluidic devices capable of generating gaseous microenvironments, including: oxygen and carbon dioxide, have also been reported.<sup>19–22</sup> In this article, we develop a microfluidic device capable of generating NO gradients based on spatially controlled chemical reactions.<sup>23</sup> Use of chemical reactions to control NO gradients eliminates the requirements of direct chemical additions, which will perturb the cellular activities. Furthermore, without using NO gas cylinders, the setup can be greatly simplified and prevent the potential hazard from high concentration NO. In the experiments, we perform NO concentration calibrations using a NO-sensitive fluorescence dye. Also, intracellular NO concentration and  $\text{Ca}^{2+}$  concentration under NO stimulations are also characterized for demonstration. The developed device enables the control of NO spatial distribution in cellular scales without tedious instrumentation and professional operation, which provides a promising technique to quantitatively study biological roles of NO and its spatial distribution using *in vitro* cell culture models.

## MATERIALS AND METHODS

### Microfluidic device design and fabrication

The developed microfluidic device is made of polydimethylsiloxane (PDMS) due to its gas permeability, optical transparency, and biocompatibility.<sup>24</sup> The device is designed with three sets of microfluidic channels. The middle channel is exploited for cell culture, and two side channels are used for NO generation chemical reactions as shown in Fig. 1(a). The middle and side channels are separated by PDMS walls with thickness of 135  $\mu\text{m}$ . In order to generate NO, the reduction reaction of nitric acid with silver is utilized in the side channel. The chemical reaction equation is written as



The generated NO diffuses into the main channel, and generates a NO gradient in a direction perpendicular to the flow direction in the middle cell culture channel.<sup>8–10</sup>

The device can be fabricated by a standard soft lithographic replica molding process as shown in Fig. 1(b).<sup>25</sup> The mold is prepared by patterning a layer of negative tone photoresist (SU-8 2050, Microchem Corp., Newton, MA) using a conventional photolithography process. To prevent undesired bonding between PDMS and the mold, the mold is first silanized with 1H, 1H, 2H, 2H-perfluorooctyltrichlorosilane (78560-45-9, Alfa Aesar, Ward Hill, MA). The mixture of PDMS prepolymer (Sylgard 184, Dow Corning Co., Midland, MI) and curing agent with a mixing ratio 10:1 (v/v) are poured onto the mold and cured at 60 °C overnight. Before assembling the device, the inlets and outlets of the channels are punched on the PDMS layer by a biopsy punch. A silver wire with a diameter of 50  $\mu\text{m}$  is embedded in one of the side channels. Afterwards, the PDMS layer is permanently bound to a PDMS coated glass using surface oxygen plasma treatment at 90 W for 40 s (PX-250, Nordson MARCH Co., Concord, CA). Figure 1(c) shows a fabricated microfluidic device capable of generating NO gradients for cell culture.

### NO gradient characterization

In order to calibrate the NO gradient profile in the middle channel, a NO sensitive fluorescence dye, 4,5-diaminofluorescein 4-amino-5-methylamino-2',7'-difluorofluorescein (DAF-FM, Molecular Probes D-23841, Invitrogen, Carlsbad, CA) is exploited in the experiments.<sup>26,27</sup> First, a deoxygenated buffer solution is prepared by bubbling pure nitrogen gas

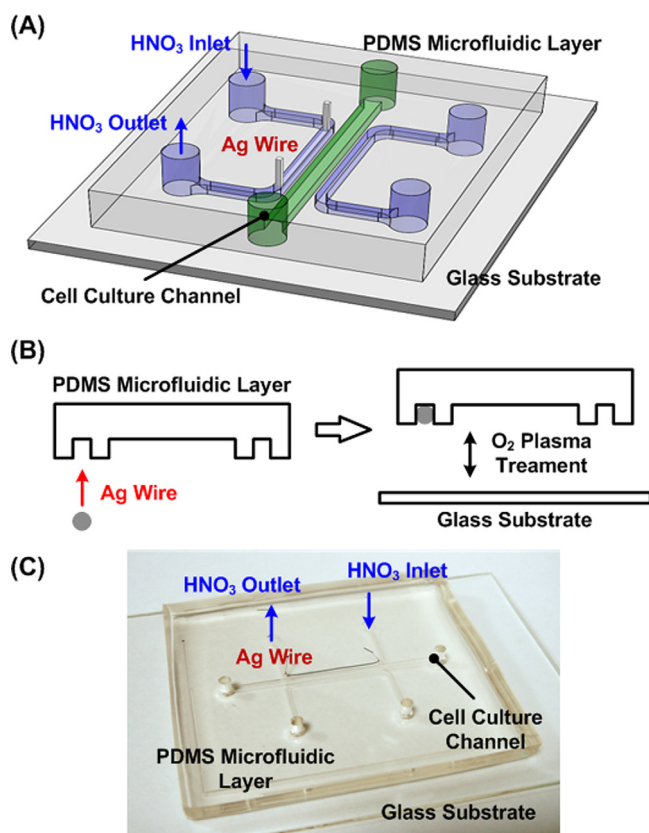


FIG. 1. (a) Illustration of the microfluidic device capable of generating NO gradients for cell culture. (b) Fabrication process of the developed microfluidic device. (c) Photo of a fabricated device.

into Dulbecco's Phosphate-Buffered Saline (DPBS, Gibco 14190, Invitrogen) for more than 30 min. Pure NO gas is then bubbled into the deoxygenated buffer solution to make a stable NO saturated solution. Solutions with four different NO concentrations ranging from 26 nM to 704 nM is prepared by serial dilution of the saturated NO solution (1.9 mM). For the fluorescence detection, the NO solutions are mixed with 7  $\mu$ M DAF-FM with a volumetric mixing ratio of 1:1. The NO calibration solutions are then injected into the middle microfluidic channel with a flow rate of 1  $\mu$ l/min using a syringe pump for fluorescence intensity measurement. To characterize NO gradients in the middle cell culture channel using the spatially confined chemical reactions, HNO<sub>3</sub> with various concentrations are introduced into the left side channel with a flow rate of 10  $\mu$ l/min while flowing the DAF-FM solutions into the middle channel with a flow rate of 1  $\mu$ l/min.

### Cell culture

NO has been intensively studied as vasodilator to relax vascular smooth cells, and how these cells response to NO is also essential to cardiovascular disease research.<sup>28–30</sup> Therefore, aortic smooth muscle cells (AoSMCs, CC-2571, Lonza, Walkersville, MD) are utilized in this study to demonstrate the device capability for cell culture studies under generated NO gradients. AoSMCs are cultured using SmGM-2 BulletKit (CC-3182, Lonza). In order to monitor intracellular NO concentrations, the AoSMCs are incubated with the 5  $\mu$ M DAF-FM diacetate (D-23844, Invitrogen) in DPBS (Gibco 14040, Invitrogen) for 1 h at 37 °C according to the manufacture's protocol for NO indicator uptake.<sup>27</sup> The cells are washed with growth medium to remove excess probes, and then incubated for additional 30 min to allow complete de-esterification of the intracellular diacetate.

### Intracellular calcium measurement

To further demonstrate using the developed device for cell studies, measurement of intracellular calcium concentration of AoSMC is performed. A ratiometric calcium-sensitive fluorescent protein, Premo<sup>TM</sup> cameleon calcium sensor (P36207, Invitrogen), is exploited to monitor  $\text{Ca}^{2+}$  flux within the cells under NO gradients.<sup>31</sup> The cells are prepared according to the manufacturer's protocol. In brief, the AoSMCs to be transduced are plated in a T25 culture flask (Nunc 136196, Thermo Fisher Scientific Inc., Penfield, NY) and allowed to adhere and grow in a 37 °C and 5%  $\text{CO}_2$  humidified cell incubator for overnight before proceeding with the transduction. The transduction solution (1 ml of cameleon calcium sensor component A and 1.75 ml DPBS) is added into the cell culture flask, and the cells are incubated at room temperature for 2 h with gentle rocking. The transduction solution is then replaced by 5 ml culture medium with 5  $\mu\text{l}$  Premo<sup>TM</sup> enhancer (component B), and the cells are then incubated in the incubator for 2 h. Afterwards, the enhancer is replaced by the normal growth medium, and the cells are cultured in the incubator for more than 16 h to allow expression of the cameleon sensor. The cells are trypsinized and seeded in the middle channel of the developed microfluidic device for the experiments. The device is placed in the cell incubator for overnight culture before the experiments.

To image the intracellular  $\text{Ca}^{2+}$  concentration variation, the cells seeded inside the device is maintained in 10x Hanks' Balanced Salt Solution (HBSS, 14065-056, Invitrogen) with 20 mM HEPES (H3784, Sigma-Aldrich, St. Louis, MO) and 2 g/l D-glucose (G8727, Sigma-Aldrich) at pH 7.4 with a flow rate of 1  $\mu\text{l}/\text{min}$ .<sup>31</sup> An inverted fluorescence microscope with Förster Resonance Energy Transfer (FRET) capability (AF7000, Leica Microsystems, Wetzlar, Germany) is exploited for observation. The excitation light with wavelength of 380–445 nm is utilized to excite cameleon calcium sensor, and the fluorescence of cyan fluorescent protein (CFP) for  $\text{Ca}^{2+}$ -unbound form is detected at the wavelength of 460–500 nm. When the sensor is bound to  $\text{Ca}^{2+}$ , FRET occurs from CFP to yellow fluorescent protein (YFP). Therefore, the sensor emits additional fluorescence at the wavelength of 525–560 nm from the YFP. As a result, the intracellular calcium concentration can be characterized by the fluorescence intensity ratio between YFP and CFP.<sup>27</sup>

## RESULTS AND DISCUSSION

### NO gradient characterization

After reacting with nitric oxide, the fluorescence quantum yield of DAF-FM is greatly enhanced about 160-fold. Figure 2(a) shows the distinct intensity profiles of the NO calibration solutions across the width of the middle channel (x-direction). The intensity profiles are obtained by analyzing fluorescence images of DAF-FM flowing in the cell culture channel detected by an inverted fluorescence microscope (AF7000, Leica Microsystems) equipped with a CCD camera (ORCA-R2, Hamamatsu Photonics, Shizuoka, Japan). Analyzing the relation between the fluorescence intensities and the solutions with known NO concentrations in every position, the NO concentration profiles can be estimated from the measured DAF-FM fluorescence intensities. Figure 2(b) shows an example of the relation between fluorescence intensities and NO concentrations at a specific position (200  $\mu\text{m}$  away from the channel wall close to the chemical reaction channel). As a result, the NO concentrations in the middle channel when introducing 12%  $\text{HNO}_3$  into the chemical reaction channel can be estimated by measuring fluorescence intensities of DAF-FM flowing in the middle channel. For example, at position  $x = 200 \mu\text{m}$ , the measured DAF-FM intensity is 1868, which represents approximately 160 nM NO by interpolating the calibration curve as shown in Fig. 2(b). As a result, the NO gradients across the width of the middle channel when introducing  $\text{HNO}_3$  with various concentrations for NO generation chemical reactions can be characterized as shown in Fig. 2(c). The results show that the NO gradients within physiological NO concentration range can be successfully generated using the device.

To understand variations of the generated NO gradients in the flow direction (y-direction), the NO gradient profiles in upstream, midstream, and downstream regions are estimated

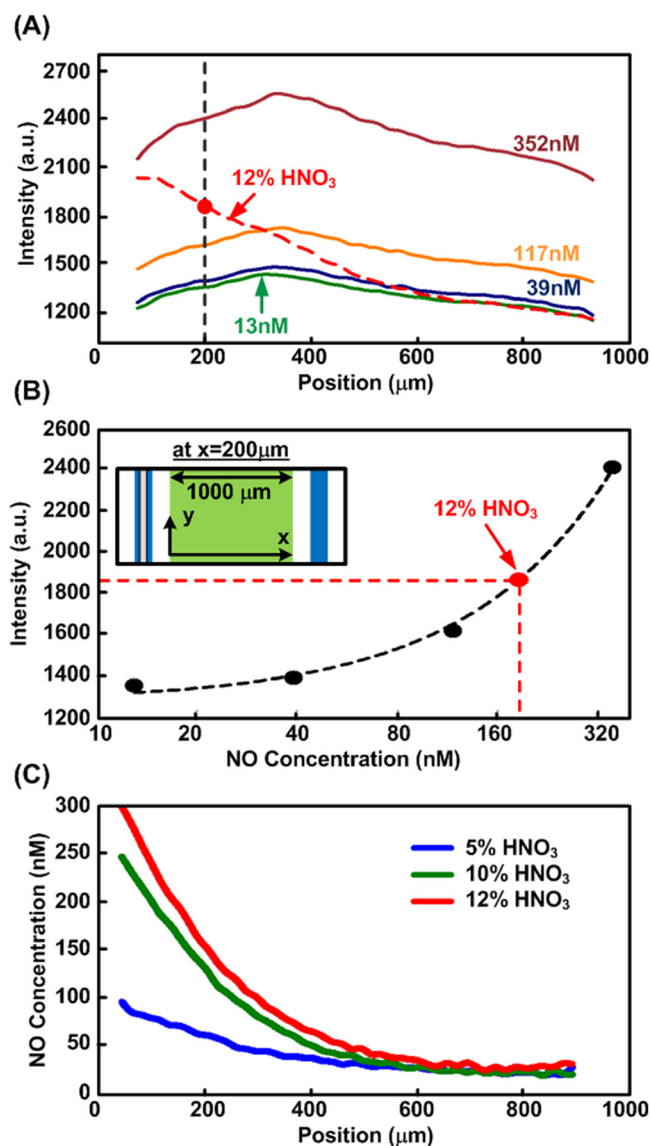


FIG. 2. (a) Experimental fluorescence intensity profiles of DAF-FM along the width of cell culture channel when introducing solutions with various NO concentrations for calibration (solid lines). The dashed line is the fluorescence profile of DAF-FM when flowing 12%  $\text{HNO}_3$  into left side channel and reacting with silver wire to produce NO. The intensity profiles are analyzed from the fluorescence images collected by an inverted fluorescence microscope equipped with a CCD camera. (b) Fluorescence intensity versus NO concentration at the position  $x = 200 \mu\text{m}$  in the cell culture channel. The concentration of NO generated using the spatially controlled chemical reaction at the position can be estimated by interpolation. (c) The resulted NO concentration profiles estimated from the calibration measurements when flowing  $\text{HNO}_3$  with different concentrations into the side channel.

according to the aforementioned procedures. Fig. 3(a) shows that the calculated NO gradients located in the three different regions are similar to each other with NO concentration differences less than 10.3 nM. Furthermore, in order to estimate the NO concentration variation in the channel height direction (z-direction), finite element analysis (FEA) is conducted using the COMSOL Multiphysics 4.3b software (COMSOL Inc., Burlington, MA). In the software, a three-dimensional model with microfluidic channels and PDMS walls is constructed, and the convection-diffusion equation is solved numerically. For the fluid field simulation, constant flow rate and no-slip boundary conditions are assigned at the inlet and the walls of the cell culture channel, respectively. For the NO diffusion simulation, constant flux boundary



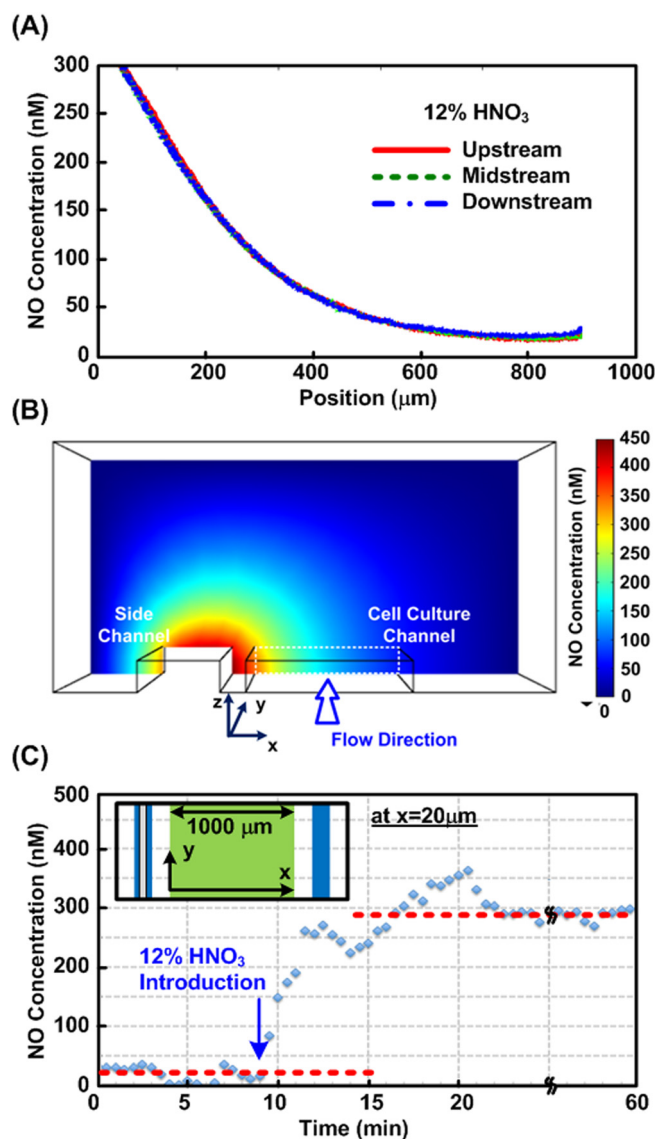


FIG. 3. (a) The experimentally measured NO gradients located at upstream, midstream, and downstream in the cell culture channel when introducing 12%  $\text{HNO}_3$  into the side channel. (b) Cross-sectional view of the constructed 3D FEA model in COMSOL Multiphysics 4.3b, and the simulation result. (c) The measured 30-s average NO concentrations at the position  $x = 20\mu\text{m}$  before and after introducing 12%  $\text{HNO}_3$  into the side channel.

conditions are applied on the chemical reaction channel walls. Figure 3(b) shows the cross-sectional view of the model constructed in the software and the simulated NO concentration profile while the liquid in the cell culture channel flows at a flow rate of  $1\mu\text{l}/\text{min}$ . The result shows that NO concentrations in the channel height direction are uniform with differences less than 10 nM.

In addition, the temporal response of the device for NO gradient generation is also studied. Fig. 3(c) shows 30-s average NO concentrations at a specific position ( $20\mu\text{m}$  away from the channel wall close to the chemical reaction channel) before and after introducing  $\text{HNO}_3$  into the side channel for NO generation at the 9th min. The NO concentration can be elevated to a desired level within 10 min and kept stable for more than 40 min. The results suggest that the developed device can efficiently generate stable NO gradients along the flow direction in the cell culture channel, which are desired for various cell culture studies.

### Intracellular NO measurement

Figures 4(a) and 4(b) show the fluorescence images of cells cultured in the middle channel with medium flow rate at  $1\ \mu\text{l}/\text{min}$  before and 30 min after introducing 12%  $\text{HNO}_3$  at flow rate of  $10\ \mu\text{l}/\text{min}$  into the side channel. It can be observed that the fluorescence intensity within cells on the left side is higher than that on the right side. Figure 4(c) plots an intensity profiles across the channel width. The result shows that the fluorescence intensity within a cell on the left side is enhanced approximately 2.1 times after exposed to NO generated by the chemical reaction. In contrast, the fluorescence intensity within a cell on the right side is similar to that before the NO exposure. The experimental result demonstrates that a NO gradient can be successfully generated in the middle cell culture channel in the direction perpendicular to the flow direction, and the intracellular NO concentrations are affected by the gradient. Moreover, the cell numbers before and after the NO gradient applications from 3 different experiments are also characterized. The number differences are less than 3.2%, which suggests the cells can attach well on the substrate after exposing to NO gradients during the experiments.

### Intracellular calcium measurement

In the experiments, 12%  $\text{HNO}_3$  is introduced into the side channel at flow rate of  $10\ \mu\text{l}/\text{min}$  and reacts with the embedded silver wire for NO gradient generation inside the middle channel to investigate its effect on intracellular  $\text{Ca}^{2+}$  concentration variations. Figure 5 shows the intracellular  $\text{Ca}^{2+}$  concentration measurement results. Figures 5(a) and 5(b) show the bright-field phase and ratiometric (YFP/CFP) microscopic images of the AoSMC cells cultured inside the

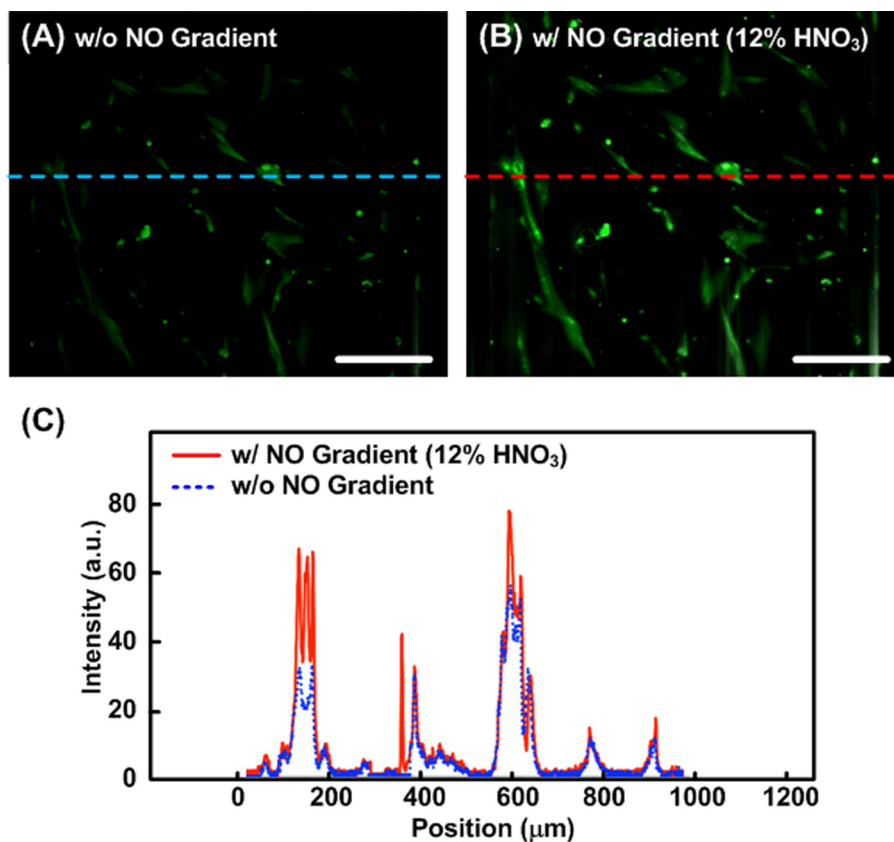


FIG. 4. Fluorescence microscopic images of AoSMCs stained with DAF-FM diacetate for intracellular NO monitoring under (a) control condition, and (b) NO gradients generated by introducing 12%  $\text{HNO}_3$  into the left side channel. (c) The fluorescence intensity profiles across the width of the cell culture channel at a specific position along the flow direction before and after introducing 12%  $\text{HNO}_3$  into the left side channel. Scale bar is  $250\ \mu\text{m}$ .

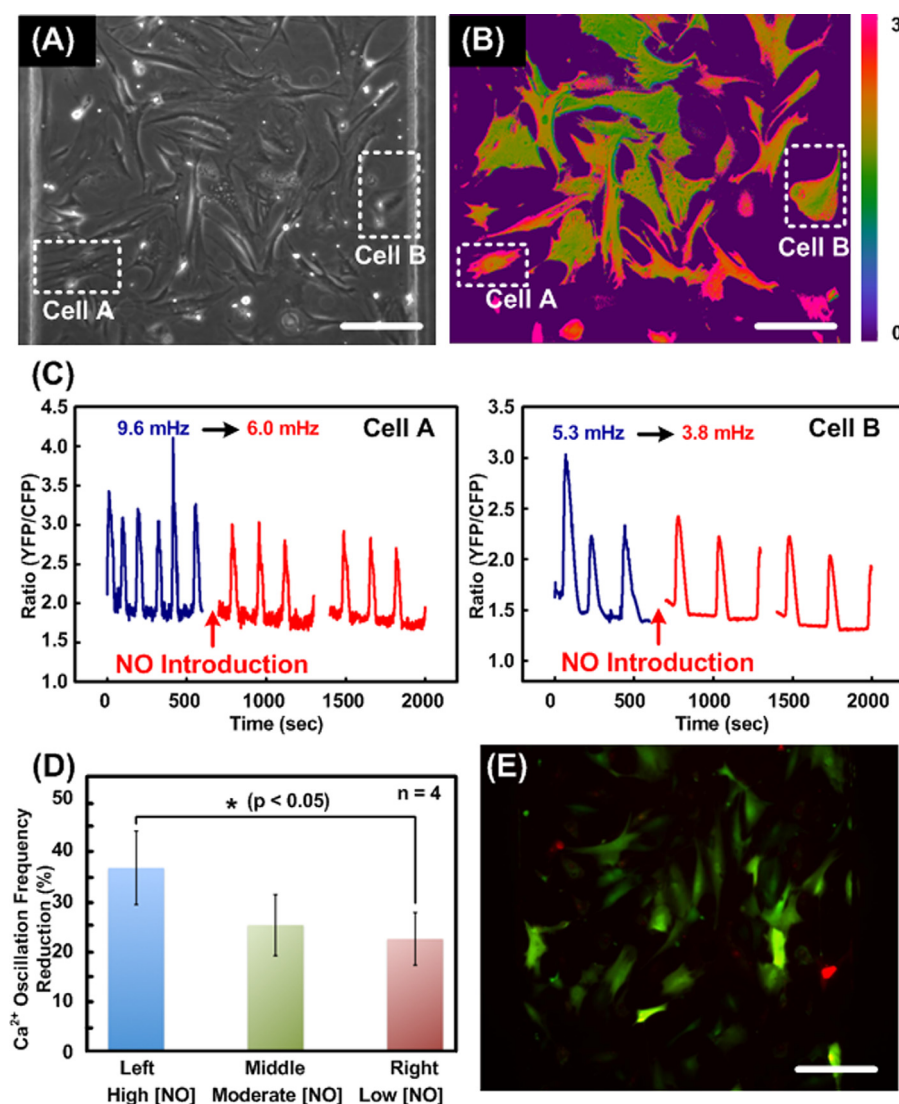


FIG. 5. (a) and (b) Bright field and FRET colormetric images of AoSMCs cultured inside the cell culture channel. (c) Measurement results of intracellular  $\text{Ca}^{2+}$  concentration oscillation within the cultured AoSMCs using FRET located in the different positions in the cell culture channel. (d) Comparison of the  $\text{Ca}^{2+}$  concentration oscillation frequency reduction of the cells located in the different positions before and after the NO stimulation. Data are expressed as the mean  $\pm$  standard deviation. (e) Fluorescence image showing cell viabilities after exposure to NO gradients for approximately 40 min. Scale bar is 200  $\mu\text{m}$ .

middle channel. To investigate the intracellular  $\text{Ca}^{2+}$  concentration variation under different NO concentrations,  $\text{Ca}^{2+}$  concentrations within a cell closed to (Cell A) and a cell far away from (Cell B) the NO generation channel are analyzed. Figure 5(c) plots the  $\text{Ca}^{2+}$  concentration variation in time domain within the cells. The results show that  $\text{Ca}^{2+}$  concentration oscillation frequencies of both cells are decreased after introducing  $\text{HNO}_3$  into the side channel for NO gradient generation. The oscillation frequency of the Cell A reduced from 9.6 mHz to 6.0 mHz ( $\sim 39.4\%$  reduction), and the oscillation frequency of the Cell B reduced from 5.3 mHz to 3.8 mHz ( $\sim 28.3\%$  reduction) after exposure to the NO gradient. Furthermore, to statistically study the  $\text{Ca}^{2+}$  concentration oscillation frequency reduction, four cells located in left, middle, and right one thirds of the channel are analyzed. An unpaired, two-tailed Student's t-test is also performed to compare the difference between the three sets of cells. Fig. 5(d) plots the  $\text{Ca}^{2+}$  oscillation frequency reduction of the three sets of cells. The cells located on the left one third of the channel, which experience higher NO concentration, have larger oscillation frequency



reduction (average 36.4%) than those located in the middle one third (average 24.8%,  $p > 0.05$ ) and right one third of the channel (average 22.1%,  $p < 0.02$ ). The results demonstrate that the NO generated using the developed method affects the intracellular  $\text{Ca}^{2+}$  concentration oscillation of the cultured AoSMCs. The demonstrated decrease of the  $\text{Ca}^{2+}$  concentration oscillation frequency has been reported to result in NO-induced smooth muscle cell relaxation.<sup>32</sup>

To further confirm the cell viability after the experiments, the fluorescence cell viability assay (LIVE/DEAD Viability/Cytotoxicity Kit, L3224, Invitrogen) is performed on the cells after the intracellular  $\text{Ca}^{2+}$  concentration observation experiments (exposure to gradients for approximately 40 min). In Figure 5(e), fluorescence image shows the cells labeled with live (green)/dead (red) stains after exposure to the NO gradient. The fluorescence image demonstrates that most the cells (>92%) are live after exposure to the physiological-level of NO generated by the developed device. The results suggest that the possible cytotoxicity of  $\text{NO}_2$ , which may be generated from oxidizing the generated NO within the physiological range, may not be a major concern in the developed microfluidic device.<sup>2</sup> Furthermore, the pH of the medium in the middle channel is monitored at the outlet during the experiments. No noticeable pH variation has been observed, which suggests the acidification of the medium by the  $\text{HNO}_3$  flowing in the neighboring channel is negligible. Consequently, the developed device provides a stable, robust, and cost-effective platform to study cellular responses under characterized NO gradients.

## CONCLUSION

In conclusion, this paper reports a microfluidic device capable of efficiently generating stable NO gradients using spatially controlled chemical reactions. The device is constructed using an elastomer material, PDMS, with great gas permeability. The chemical reaction between nitric acid and silver is exploited to generate NO. In the experiments, NO concentration profiles are characterized using NO-sensitive fluorescence dye, DAF-FM. Furthermore, AoSMCs are cultured inside the device to demonstrate the device performance for cell culture studies. The intracellular NO concentration and  $\text{Ca}^{2+}$  concentration variation are characterized under NO gradients. The results demonstrate the device can be exploited to study cell behaviors under various physiological level NO concentrations. Without bulky and highly hazardous NO gas cylinders, the device provides a simple, straightforward, and safe experimental setup to study the roles of NO on *in vitro* cell models. In addition, without direct addition of NO donor, the cellular activities will not be affected by the undesired chemical reactants. Moreover, taking advantages the methods developed in this paper, it is also possible to construct a cell culture array platform with various uniformly distributed NO concentrations for toxicity or mutagenesis assays without tedious and complex instrumentation.<sup>33</sup> The device may pave the ways for researchers to better study the biological roles of NO in various cellular and tissue responses, which has been a challenging task for decades.

## ACKNOWLEDGMENTS

The authors gratefully thank Mr. Chueh-Yu Wu for the fruitful discussion, and the support from the National Health Research Institutes (NHRI) in Taiwan under Career Development Grant (CDG) (EX102-10021EC), National Science Council (NSC) in Taiwan under Grant NSC 101-2628-E-001-002-MY3, and the Academia Sinica Research Program on Nanoscience and Nanotechnology.

<sup>1</sup>D. S. Bredt and S. H. Snyder, *Annu. Rev. Biochem.* **63**, 175 (1994).

<sup>2</sup>J. S. Beckman and W. H. Koppenol, *Am. J. Physiol.* **271**, C1424 (1996).

<sup>3</sup>R. M. J. Palmer, A. G. Ferrige, and S. Moncada, *Nature* **327**, 524 (1987).

<sup>4</sup>S. Moncada, R. M. Palmer, and E. A. Higgs, *Pharmacol. Rev.* **43**, 109 (1991).

<sup>5</sup>C. Wang and W. M. Deen, *Ann. Biomed. Eng.* **31**, 65 (2003).

<sup>6</sup>A. G. Estevez, N. Spear, H. Pelluffo, A. Kamaid, L. Barbeito, and J. S. Beckman, *Methods Enzymol.* **301**, 393 (1999).

<sup>7</sup>A. Gasco, R. Fruttero, and G. Sorba, *Farmacognosia* **51**, 617 (1996).

<sup>8</sup>M. Kavdia, S. Nagarajan, and R. S. Lewis, *Chem. Res. Toxicol.* **11**, 1346 (1998).

<sup>9</sup>R. S. Lewis and W. M. Deen, *Chem. Res. Toxicol.* **7**, 568 (1994).

- <sup>10</sup>A. Ramamurthi and R. S. Lewis, *Ann. Biomed. Eng.* **26**, 1036 (1998).
- <sup>11</sup>J. N. Bates, M. T. Baker, R. Guerra, Jr., and D. G. Harrison, *Biochem. Pharmacol.* **42**, S157 (1991).
- <sup>12</sup>S. Kashiwagi, K. Tsukada, L. Xu, J. Miyazaki, S. V. Kozin, J. A. Tyrrell, W. C. Sessa, L. E. Gerweck, R. K. Jain, and D. Fukumura, *Nat. Med.* **14**, 255 (2008).
- <sup>13</sup>N. L. Jeon, H. Baskaran, S. K. Dertinger, G. M. Whitesides, L. van de Water, and M. Toner, *Nat. Biotechnol.* **20**, 826 (2002).
- <sup>14</sup>J. W. Song, W. Gu, N. Futai, K. A. Warner, J. E. Nor, and S. Takayama, *Anal. Chem.* **77**, 3993 (2005).
- <sup>15</sup>Y. Kamotani, T. Bersano-Begey, N. Kato, Y.-C. Tung, D. Huh, J. W. Song, and S. Takayama, *Biomaterials* **29**, 2646 (2008).
- <sup>16</sup>C. Moreas, J. H. Chen, Y. Sun, and C. A. Simmons, *Lab Chip* **10**, 227 (2010).
- <sup>17</sup>N. J. Douville, P. Zamankhan, Y.-C. Tung, R. Li, B. L. Vaughan, C.-F. Tai, J. White, P. J. Christensen, J. B. Grotberg, and S. Takayama, *Lab Chip* **11**, 609 (2011).
- <sup>18</sup>M.-C. Liu, H.-C. Shih, J.-G. Wu, T.-W. Weng, C.-Y. Wu, J.-C. Lu, and Y.-C. Tung, *Lab Chip* **13**, 1743 (2013).
- <sup>19</sup>G. Mehta, J. Lee, W. Cha, Y.-C. Tung, J. J. Linderman, and S. Takayama, *Anal. Chem.* **81**, 3714 (2009).
- <sup>20</sup>M. Pinelis, L. Shamban, A. Jovic, and M. M. Maharbiz, *Biomed. Microdevices* **10**, 807 (2008).
- <sup>21</sup>M. Adler, M. Polinkovsky, E. Gutierrez, and A. Groisman, *Lab Chip* **10**, 388 (2010).
- <sup>22</sup>A. Takano, M. Tanaka, and N. Futai, *Microfluid. Nanofluid.* **12**, 907 (2012).
- <sup>23</sup>Y.-A. Chen, A. D. King, H.-C. Shih, C.-C. Peng, C.-Y. Wu, W.-H. Liao, and Y.-C. Tung, *Lab Chip* **11**, 3626 (2011).
- <sup>24</sup>M. A. Eddings and B. K. J. Gale, *J. Micromech. Microeng.* **16**, 2396 (2006).
- <sup>25</sup>Y. Xia and G. M. Whitesides, *Annu. Rev. Mater. Sci.* **28**, 153 (1998).
- <sup>26</sup>H. Kojima, N. Nakatsubo, K. Kikuchi, S. Kawahara, Y. Kirino, H. Nagoshi, Y. Hirata, and T. Nagano, *Anal. Chem.* **70**, 2446 (1998).
- <sup>27</sup>H. Kojima, Y. Urano, K. Kikuchi, T. Higuchi, Y. Hirata, and T. Nagano, *Angew. Chem., Int. Ed.* **38**, 3209 (1999).
- <sup>28</sup>R. R. Fiscus, R. M. Rapoport, and F. Murad, *J. Cyclic Nucleotide Protein Phosphor Res.* **9**, 415 (1983).
- <sup>29</sup>L. J. Ignarro, R. E. Byrns, G. M. Buga, K. S. Wood, and G. Chaudhuri, *J. Pharmacol. Exp. Ther.* **244**, 181 (1988).
- <sup>30</sup>U. C. Garg and A. Hassid, *J. Clin. Invest.* **83**, 1774 (1989).
- <sup>31</sup>A. E. Palmer and R. Y. Tsien, *Nat. Protoc.* **1**, 1057 (2006).
- <sup>32</sup>J. F. Perez-Zoghbi, Y. Bai, and M. J. Sanderson, *Gen. Physiol.* **135**, 247 (2010).
- <sup>33</sup>C.-C. Peng, W.-H. Liao, Y.-H. Chen, C.-Y. Wu, and Y.-C. Tung, *Lab Chip* **13**, 3239 (2013).